Novel Preparation of Intercellular Lipid Models of the Stratum Corneum Containing Stereoactive Ceramide

Hiroshi Watanabe,[a] Yasuko Obata,*[,a] Yoshinori Onuki,[a] Kenya Ishida,[b] and Kozo Takayama[a]

[a] *Department of Pharmaceutics, Hoshi University; 2–4–41 Ebara, Shinagawa-ku, Tokyo 142–8501, Japan: and* [b] *Takasago International Corporation; 1–4–11 Nishiyawata, Hiratsuka, Kanagawa 254–0073, Japan.*

Received August 24, 2009; accepted December 5, 2009; published online December 22, 2009

The microstructure formed by intercellular lipids in the stratum corneum is important for the barrier function of the skin. However, the correlation between lipid composition and microstructure has not yet been clarified. To elucidate the microstructure of intercellular lipids in the stratum corneum, an intercellular lipid model was prepared from ceramide 5 (CER5), cholesterol (CHOL), and palmitic acid (PA), considering the nonuniformity of the lipid components of the stratum corneum. A response surface method incorporating thin-plate spline interpolation (RSM-S) was employed to prepare the CER5/CHOL/PA lipid bilayers. Fluorescence anisotropy of the CER5/CHOL/PA bilayers showed four distinct clusters based on Kohonen's self-organizing maps (SOM). At the centroid formulation of those clusters, the microstructures of CER5/CHOL/PA bilayers were determined using synchrotron X-ray scattering. Three kinds of lamellar structures and two kinds of lateral packing—namely, hexagonal and orthorhombic—were formed. The microstructure of the CER5/CHOL/PA bilayers was likely to be intrinsic to the intercellular lipids in the stratum corneum. In conclusion, the CER5/CHOL/PA bilayers prepared based on RSM-S and SOM were useful as models of the intercellular lipids in the stratum corneum.

Key words stratum corneum; ceramide; synchrotron X-ray scattering; response surface method incorporating thin-plate spline interpolation; self-organizing map

The stratum corneum, the outermost layer of the skin, plays the main barrier for the drug permeation *via* the skin. The barrier function of the stratum corneum is dominated by the microstructure formed by intercellular lipids in the stratum corneum consisting of ceramide (CER), cholesterol (CHOL), fatty acids, and their derivatives. The lipid microstructure, the molecular arrangement of intercellular lipids in the stratum corneum, has been investigated using synchrotron X-ray scattering and neutron diffraction.[1—3] Two kinds of lamellar structures were observed by small angle X-ray scattering (SAXS) and neutron diffraction. One of them is a short lamellar structure with a repeat distance of about 6 nm, and the other is a long one with a repeat distance thought to be about 13 nm.[4] On the other hand, hydrocarbon chain packing was obtained by wide angle X-ray scattering (WAXS). Hexagonal hydrocarbon chain packing with a lattice distance of about 0.42 nm and orthorhombic packing with lattice distances of about 0.42 nm and 0.37 nm have been observed.[5] The correlation between lamellar structure and hydrocarbon chain packing was investigated by simultaneous measurements using SAXS and WAXS employing differential scanning calorimetry.[6] It is assumed that these two kinds of hydrocarbon chain packing were determined by the unbalance of the lipid compositions of intercellular lipid in stratum corneum. Moreover, stratum corneum lipid components at the surface were found to be different from those at a deeper position.[7] Recently, the distribution of the lipid components and microstructures in stratum corneum was focused on the various groups to clarify the relationship between microstructure and barrier function of the skin.[8—10] But, the correlation between lipid composition and the resulting microstructure formation of intercellular lipids in the stratum corneum is not yet fully understood.

To develop the effective transdermal drug delivery systems and cosmetics, it is important to determine the characteristics of the intrinsic lipid microstructure in stratum corneum and the alteration of lipids in the stratum corneum caused by administration of components in pharmaceutical or cosmetic formulations. Although many studies have been performed to clarify the effect of chemical permeation enhancers on the lipid microstructure of the stratum corneum,[11,12] the use of natural stratum corneum is rather difficult because of its noisy background. The microstructure of stratum corneum lipids has a diversity that enables it to act as a barrier to dehydration and to the invasion of foreign hazards. A simplified model is necessary to investigate the understanding the diversity of the microstructure and the molecular interaction between the stratum corneum lipids and chemical enhancers.

Lipid mixtures of various types of CERs/CHOL/free fatty acids have been prepared as models of the intercellular lipids in the stratum corneum.[13—16] It has already been clarified that CER1 with a long chain fatty acid side chain is important for the formation of long lamellar structures.[13] Moreover, fatty acids affect the formation of orthorhombic hydrocarbon chain packing.[14] These results suggested that the composition of the intercellular lipid in stratum corneum was greatly related to the microstructure of stratum corneum lipids. However, a shortcoming of the suggested models is the singular interpretation of unvaried membrane properties. Thus, the previously proposed models cannot show the overall nature of lipid microstructure that consists of various intercellular lipid components in the stratum corneum.

The barrier function of the skin is related to the molecular arrangement of the intercellular lipid in stratum corneum. Therefore, to grasp the barrier function of the skin, it is important to elucidate the relationships between lipid compositions and organization of the intercellular lipid in stratum corneum. The purpose of this study is elucidation of the intercellular lipid models consisted of the typical hydrocarbon chain packing of the intercellular lipid in stratum corneum using the statistical approach. Generally, the correlation between phase behaviors and lipid compositions of the model

* To whom correspondence should be addressed. e-mail: obata@hoshi.ac.jp

bilayer were complicated. A few alteration of the lipid compositions caused significantly changes of the phase behavior of the lipid bilayers. Therefore, to clarify the detail phase behavior and correlation between microstructure and compositions of the lipids bilayers, enormous experiments were required. In the present study, to build a model of intercellular lipids found in the stratum corneum that considers the diversity of its lipid composition, a response surface method incorporating thin-plate spline interpolation (RSM-S) and Kohonen's self-organizing maps (SOM) were introduced.[17] RSM-S and SOM were applied to the formulation optimization of pharmaceutical products, and these techniques were useful to reveal the latent structure lagging on the optimal formulation problems.[18] At first, a ternary phase diagram for CER5, CHOL, and palmitic acid (PA) was arranged to choose distinct models of the intercellular lipids in the stratum corneum. These species are typical components in stratum corneum lipid. It is suggested that the lipid bilayer that consisted of these lipids can partially reproduce the microstructure of the intercellular lipid in stratum corneum.[14] To evaluate the characteristics of these lipid models, the fluidity and microstructure in those models was evaluated by fluorescence anisotropy and synchrotron X-ray scattering. In the stratum corneum, CER2, CER5, and CER7 constitute about 20% of the intercellular lipids.[19,20] In this study, CER5 was selected as the main CER component in the model membranes.

Experimental

Materials (2*S*,3*R*)-2-(2-Hydroxyhexadecanoyl)aminooctadecane-1,3-diol (95%) (Ceramide 5) was supplied by Takasago International (Tokyo, Japan). Cholesterol (99%), palmitic acid (99%) and 1,6-diphenyl-1,3,5-hexatriene (DPH; 98%) were purchased from Sigma-Aldrich (St. Louis, MO, U.S.A.). Human stratum corneum sheet was purchased from Biopredic International (Rennes, France). The stratum corneum sheet was separated from the donated skin, which separated from the breast of the white woman by the cosmetic surgery, with trypsin. Chloroform and tetrahydrofuran were certified grade. Other chemicals used were reagent grade.

Preparation of CER5/CHOL/PA Bilayers Ceramide 5, CHOL, and PA (CER5/CHOL/PA) bilayers were prepared as reported previously.[21] The molar ratio of CER5 was 10—50 mol%, CHOL was 0—80 mol%, and PA was 10—90 mol%. In brief, the designated amounts of lipids dissolved in chloroform/methanol (2 : 1) were transferred into a flask using a pipette, and the solvent was removed by evaporation at room temperature under a stream of nitrogen. This procedure resulted in the formation of a thin lipid film on the inside wall of the flask. Acetate buffer (10 ml, pH 5.0) was added to the flask, and the lipids were hydrated for 30 min. The suspension was sonicated for 5 min at above the phase transition temperature using a bath-type sonicator. The CER5/CHOL/PA bilayer suspension was prepared to produce a total lipid concentration of 10 mM and stored at room temperature until used in the experiments.

Preparation of Human Stratum Corneum Sheet The human stratum corneum sheet was rinsed in purified water and dried *in vacuo*. The stratum corneum was incubated with purified water for 12 h at ambient temperature and dried under a stream of nitrogen until it reached an acceptable weight (125% of dried weight).

Fluorescence Anisotropy Measurements The CER5/CHOL/PA bilayer was labeled with DPH by adding 10 μl of freshly prepared 10 mM DPH stock solution in tetrahydrofuran to 1 ml of CER5/CHOL/PA bilayer suspension and then incubated at 37 °C for 2 h in the dark to complete the labeling. The fluorescence anisotropy of DPH in the CER5/CHOL/PA bilayers was measured using a fluorescence spectrophotometer (F-7000, Hitachi, Tokyo, Japan) at an excitation wavelength of 351 nm and an emission wavelength of 430 nm. The fluorescence anisotropy was calculated using the following equation:

$$A = \frac{I_0 - G \times I_{90}}{I_0 + 2G \times I_{90}}$$

where A is anisotropy, I_0 and I_{90} are the intensity measured in directions parallel and perpendicular to polarized exciting light, and G is instrumental constant.

Data Analysis dataNESIA® version 3.0 (Yamatake Corp., Tokyo, Japan) was used for RSM-S. Viscovery SOMine® version 5.0 (Eudaptics Software, Vienna, Austria) was used for SOM clustering. SOM software offers several clustering techniques; for example a SOM-Ward, a Ward, and a SOM-Single-Linkage. Among these techniques, the SOM Ward was applied for the clustering for the lipids membrane compositions because in general, it is considered the most efficient.

Estimation of Ternary Phase Diagram of CER5, CHOL, and PA With reference to the methods of Onuki and Takayama,[17] a ternary phase diagram was determined. The drawing up of the phase diagram was conducted using the following procedures. At first, 35 model CER5/CHOL/PA bilayers were prepared. Then, the fluorescence anisotropy of DPH in the CER5/CHOL/PA bilayers was measured with a heating scan from 25 to 70 °C at a rate of 1 °C/min. Next, the CER5/CHOL/PA bilayer compositions and the observed fluorescence anisotropy values were used as a training data set, and the response surfaces that expressed the relationship between the CER5/CHOL/PA bilayer composition and membrane fluidity were generated at 50 °C, 52 °C, 54 °C, …, and 70 °C using the RSM-S, respectively. The untested fluorescence anisotropy values were predicted by the response surfaces. The number of untested CER5/CHOL/PA bilayer compositions for the prediction was 2466. All experimental and predicted data were processed by the SOM clustering. A lipid composition and the series of fluorescene anisotropy values at different temperatures were regarded as an input data set. Namely, 2501 data sets including experimental and predicted data were used for SOM clustering. The number of nodes in output was set at 1250. Thus, a ternary phase diagram indicating the distribution of distinct membranes was estimated using reference vectors from each cluster.

Small and Wide Angle X-Ray Scattering Measurements The measurement of SAXS and WAXS profiles of CER5/CHOL/PA bilayers were carried out at the Photon Factory BL15A in the High Energy Accelerator Research Organization (Ibaraki, Japan) and human stratum corneum's profile was obtained from measurements at the BL40B2 (Structural Biology II Beamline) in SPring-8 (Hyogo, Japan). The wavelength (λ) of the X-ray beam was about 0.151 nm, and the sample-to-detector distances were about 1600 mm (SAXS) and 160 mm (WAXS). The reciprocal spacing $S = 1/d = (2/\lambda)\sin(2\theta/2)$ was calibrated from the lattice spacing of plumbum stearate crystal at room temperature, where 2θ is the scattering angle, and d is the lattice distance. A sample cell containing the CER5/CHOL/PA membrane suspension or human stratum corneum was sealed with a polyimide film and placed in the sample holder of the X-ray diffractometer. The sample temperature was controlled at 35 °C using a differential scanning calorimetry (FP-99; Mettler-Toledo, Tokyo, Japan).

Results

Preparation of the CER5/CHOL/PA Bilayers as a Model of Intercellular Lipids in the Stratum Corneum

Fluorescence anisotropy is considered to be a method for assessing membrane fluidity. The fluidity of membranes is related to the barrier function of the skin.[19] Therefore, fluorescence anisotropy is a useful parameter for the investigation of the phase behavior of the CER5/CHOL/PA bilayers. The fluorescence anisotropy spectra obtained in the model bilayers were remarkably different according to the bilayer lipid composition. To generate the response surfaces at various temperatures, RSM-S was applied to the fluorescence anisotropy values. Figure 1 shows response surfaces at 50 °C, 60 °C, and 70 °C generated by RSM-S. The fluorescence anisotropy values at 50 °C were similar to those at 60 °C. However, the values at 70 °C were greatly different from those at 50 °C or 60 °C. Furthermore, the values were drastically changed depending on the lipid composition. SOM clustering was applied to the data of 2501 experimental and predicted compositions, and CER5/CHOL/PA bilayers were classified into four clusters (Fig. 2). For instance, cluster 1 was summarized as a PA-rich group, but cluster 4 was considered to be a group having a low molar ratio of PA and a high molar ratio

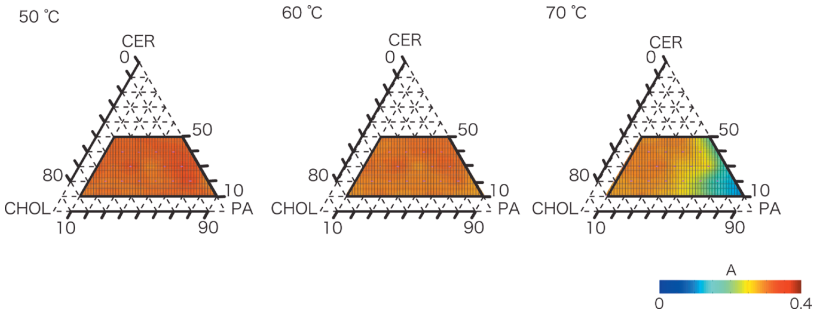

Fig. 1. Ternary Phase Diagrams of Fluorescence Anisotropy Values in CER5/CHOL/PA Bilayers Generated by RSM-S at 50 °C, 60 °C, and 70 °C

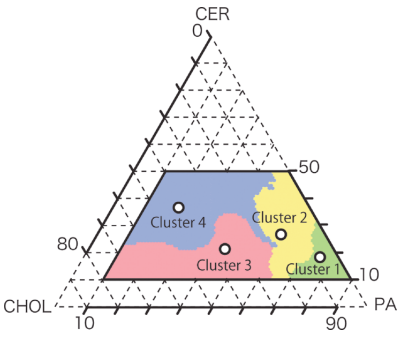

Fig. 2. Clusters of CER5/CHOL/PA Classified Based on SOM Clustering

Open circles indicate the centroids in each cluster.

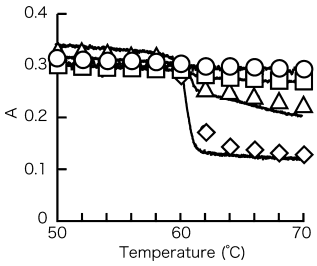

Fig. 3. Fluorescence Anisotropy of the DPH in Typical CER5/CHOL/PA Bilayers Belonging to Each Cluster

Symbols (◇, △, □, and ○) represent the predicted fluorescence anisotropy values determined by RSM-S and SOM clustering, and the line represents the experimental values. Cluster 1 (◇), cluster 2 (△), cluster 3 (□), and cluster 4 (○).

Table 1. The Centroid Formulation of CER5/CHOL/PA Bilayers Belonging to Each Cluster Estimated by the RSM-S and SOM Clustering[a)]

	CER	CHOL	PA
Cluster 1	17.8	5.5	76.6
Cluster 2	26.5	13.9	59.6
Cluster 3	21.0	35.1	43.9
Cluster 4	36.6	42.8	20.6

a) mol%.

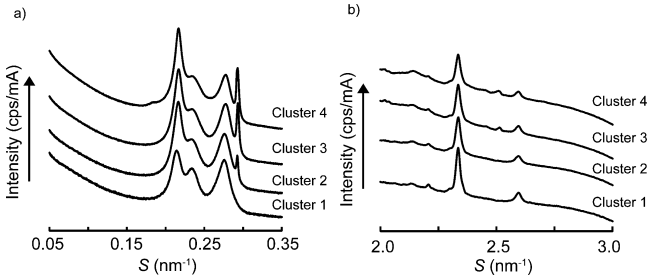

Fig. 4. Synchrotron X-Ray Scattering Profile of Typical CER5/CHOL/PA Bilayers Belonging to Each Cluster

(a) The profile of SAXS and (b) the profile of WAXS. The reciprocal spacing is indicated by the formula: $S=n\lambda/2\sin\theta$, where λ is the wavelength of the X-ray, n is the degree of scattering, and θ is the scattering angle.

of CHOL. The centroids of each cluster were selected as representative of the four lipid bilayer groups. The centroid formulations of CER5/CHOL/PA bilayers in the clusters are summarized in Table 1.

The Membrane Properties and Microstructure of CER/CHOL/PA Bilayers Figure 3 shows the fluorescence anisotropy of the CER5/CHOL/PA bilayers in each cluster as a function of temperature. The predicted values were in good agreement with corresponding experimental values ($R^2=0.964$) suggesting that the ternary phase diagram generated by RSM-S and SOM clustering represented the relationship between the membrane compositions and fluorescence anisotropy values. The fluorescence anisotropy value at cluster 1 was significantly decreased at 62 °C. With an increasing molar ratio of CHOL, the change in the fluorescence anisotropy profiles became smaller. In cluster 4, where the membrane composition consisted of a high molar ratio of CER5 and CHOL, no change in fluorescence anisotropy was seen in the temperature range of 50 °C to 70 °C. Therefore, this suggested that the microstructure of CER5/CHOL/PA bilayers was greatly changed depending on their membrane composition.

The results obtained from the SAXS and WAXS measurements are shown in Fig. 4. In SAXS measurements (Fig. 4a), the CER5/CHOL/PA bilayers in each cluster indicated three diffraction peaks; the repeat distances were 4.65 nm ($S=0.215\,\mathrm{nm}^{-1}$), 4.38 nm ($S=0.228\,\mathrm{nm}^{-1}$), and 3.62 nm ($S=0.276\,\mathrm{nm}^{-1}$), respectively. The repeat distances 4.65 nm and 3.62 nm were defined as the long and short lamellar structures, respectively. A diffraction peak whose repeat distance was 3.42 nm ($S=0.292\,\mathrm{nm}^{-1}$) appeared in clusters 2, 3, and 4. The diffraction patterns observed with WAXS measurements are shown in Fig. 4b. The two diffraction peaks appeared where lattice distances in hydrocarbon chain packing were 0.429 nm ($S=2.33\,\mathrm{nm}^{-1}$) and 0.378 nm ($S=2.58\,\mathrm{nm}^{-1}$). These two peaks represent the hexagonal and orthorhombic hydrocarbon chain packing in CER5/CHOL/PA bilayers in each cluster. Moreover, in the case of clusters 2, 3, and 4, the weaker diffraction appeared where $S=0.250\,\mathrm{nm}^{-1}$. This peak correlated with the diffraction at $S=0.292\,\mathrm{nm}^{-1}$ in SAXS

measurement. Those diffraction peaks might have arisen from CHOL.

The Microstructure of the Human Stratum Corneum To investigate the similarity between CER5/CHOL/PA bilayers and human stratum corneum, the microstructure of the human stratum corneum was determined by the WAXS measurement. Figure 5 shows the WAXS profile of the human stratum corneum. Two distinct diffractions were appeared which lattice distances were 0.416 nm (S=2.40 nm^{-1}) and 0.375 nm (S=2.66 nm^{-1}). Those two diffractions represent the hexagonal and orthorhombic hydrocarbon chain packing of the intercellular lipid in stratum corneum that corresponds to the previous result.[5)]

Discussion

Using RSM-S and SOM clustering, four types of CER5/CHOL/PA bilayers were extracted from phase diagrams of CER5, CHOL, and PA as models for the intercellular lipids in the stratum corneum. The CER5/CHOL/PA bilayers formed three kinds of lamellar structure and two kinds of hydrocarbon chain packing. As indicated by the SAXS measurement, the CER5/CHOL/PA membranes formed long and short lamellar structures. The repeat distances of long and short lamellar structures were shorter than those for intrinsic intercellular lipids in the stratum corneum.[4)] The intercellular lipid in the stratum corneum consisted of the various types of CERs including *N*-(ω-hydroxyacyl)acylsphingosine. However, CER5/CHOL/PA bilayers consisted of CER5, which has a medium chain fatty acid side chain. Therefore, the difference in repeat distance appears to be derived from the differences in CER types between the intercellular lipid in the stratum corneum and the CER5/CHOL/PA bilayers. The lamellar structure with a repeat distance of about 4.38 nm might be derived from a lamellar-liquid crystal. The full width at half maximum value of the diffraction peak of this lamellar structure indicated a greater vaemellarchain packing of lipidsylue than for the long and short lamellar structures (S=0.215 nm^{-1} and S=0.276 nm^{-1}, respectively). It was suggested that molecular arrangement of the lamellar structure with a repeat distance about 4.36 nm was disordered compared with long and short lamellar structures.

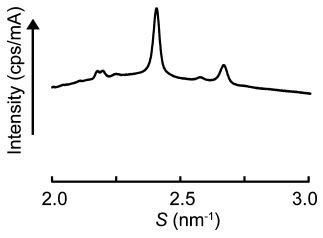

Fig. 5. WAXS Profile of the Human Stratum Corneum

The reciprocal spacing is indicated by the formula: $S=n\lambda/2\sin\theta$, where λ is the wavelength of the X-ray, n is the degree of scattering, and θ is the scattering angle.

Quantitative evaluation of the measurement of X-ray scattering was difficult in some cases. However, we attempted to determine the apparent ratio of hydrocarbon chain packing of lipid lamellae in stratum corneum.[12)] In this study, the apparent ratio of long and short lamellar structures ($R_{\mathrm{Long/Short}}$) was defined as:

$$R_{\mathrm{Long/Short}}=\frac{S_{\mathrm{Long}}}{S_{\mathrm{Short}}}$$

where S_{Long} is the integrated intensity of the diffraction peak at S=0.215 nm^{-1}, and S_{Short} is that at S=0.276 nm^{-1}. Greater $R_{\mathrm{Long/Short}}$ values indicate that long lamellar is major structure in the CER5/CHOL/PA bilayers. The difference in $R_{\mathrm{Long/Short}}$ values in each cluster is shown in Fig. 6a. The $R_{\mathrm{Long/Short}}$ value of cluster 1 was 0.965. Therefore, the apparent ratio of short lamellar structures was greater than that of long lamellar structures. With an increasing molar ratio of CHOL, $R_{\mathrm{Long/Short}}$ values became greater than in cluster 1. In the case of cluster 4, the $R_{\mathrm{Long/Short}}$ value was indicated to be 42.3. Therefore, long lamellar structures were considered to be dominant in cluster 4. On the other hand, in WAXS measurements, the apparent ratio of hexagonal/orthorhombic hydrocarbon chain packing ($R_{\mathrm{Hexa/Ortho}}$) was defined as:

$$R_{\mathrm{Hexa/Ortho}}=\frac{(S_{2.38}-2\times S_{2.70})/3}{S_{2.70}}$$

where $S_{2.38}$ is the integrated intensity of the diffraction peak at S=2.38 nm^{-1}, and $S_{2.70}$ is that of the peak at S=2.70 nm^{-1}. The denominator indicates the apparent area derived from the orthorhombic hydrocarbon chain packing and the numerator indicates the apparent area of the hexagonal hydrocarbon chain packing. $2\times S_{2.70}$ means the apparent area derived from orthorhombic hydrocarbon chain packing in the area of the diffraction peak at S=2.38 nm^{-1}. When, the hexagonal and orthorhombic hydrocarbon chain packing appear in the CER5/CHOL/PA bilayer at the equivalent ratio, the $R_{\mathrm{Hexa/Ortho}}$ value indicates 1. Greater $R_{\mathrm{Hexa/Ortho}}$ values indicate that the hexagonal hydrocarbon chain packing is dominant in the CER5/CHOL/PA bilayers. The $R_{\mathrm{Hexa/Ortho}}$ values of CER5/

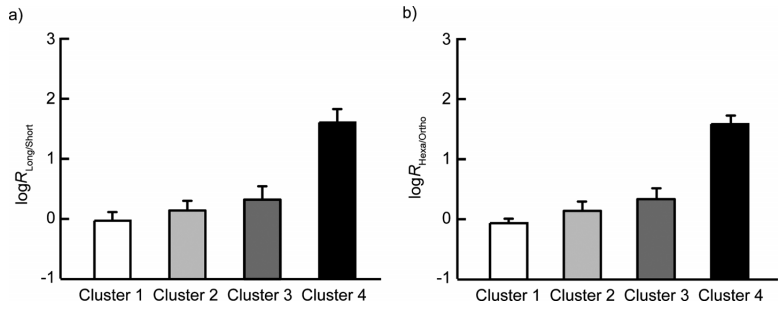

Fig. 6. The Apparent Ratio of the Microstructure in Typical CER5/CHOL/PA Bilayers Belonging to Each Cluster

(a) The apparent ratio of the long lamellar structure with a repeat distance of about 4.65 nm and long lamellar structure with a repeat distance about 3.62 nm and (b) the apparent ratio of the hexagonal and orthorhombic hydrocarbon chain packing. Each column represents the mean±S.D. (n=3).

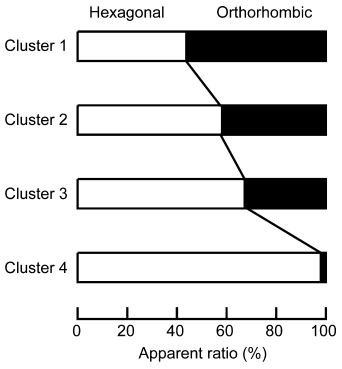

Fig. 7. A Summary of the Microstructure of CER5/CHOL/PA Bilayers in Each Cluster

The open and closed bars represent the hexagonal and orthorhombic hydrocarbon chain packing, respectively.

CHOL/PA bilayer in each cluster are shown in Fig. 6b. The $R_{\text{Hexa/Ortho}}$ value of cluster 1 indicated 0.894. In cluster 1, the orthorhombic hydrocarbon chain packing was considered to be the principal type. With an increase in the molar ratio of CHOL, $R_{\text{Hexa/Ortho}}$ values were increased. In clusters 2 and 3, the apparent ratio of hexagonal hydrocarbon chain packing was increased. The $R_{\text{Hexa/Ortho}}$ value of cluster 4 was 40.8. This value indicated that about 98% of hydrocarbon chain packing in the CER5/CHOL/PA bilayer in the cluster 4 composed of the hexagonal hydrocarbon chain packing. Thus, hexagonal hydrocarbon chain packing was dominant in the CER5/CHOL/PA bilayer of cluster 4. The microstructure of CER5/CHOL/PA bilayers is summarized in Fig. 7. The apparent ratio of the hydrocarbon chain packing was altered according to the difference of formulations. The change in the $R_{\text{Hexa/Ortho}}$ values was similar to that in the $R_{\text{Long/Short}}$ values in the same cluster. These results suggest that the hexagonal hydrocarbon chain packing is composed of long lamellar structures and orthorhombic packing is characteristic of short lamellar structures. The CER5/CHOL/PA bilayers might consist of two kinds of lipid domains, those with hexagonal and those with orthorhombic hydrocarbon chain packing. Moreover, the differences in the microstructure of the CER5/CHOL/PA bilayers were attributable to the components of the lipid membranes. The CER5/CHOL/PA bilayer in cluster 1 consisted of a high molar ratio of PA and predominantly formed orthorhombic hydrocarbon chain packing. In contrast, the CER5/CHOL/PA bilayer in cluster 4 mainly consisted of a low molar ratio of PA and formed hexagonal hydrocarbon chain packing. The results suggested that CER5- and CHOL-rich membranes consisted of hexagonal hydrocarbon chain packing. On the other hand, the formation of orthorhombic hydrocarbon chain packing was induced by the presence of a greater amount of PA in the CER5/CHOL/PA bilayers. Previous reports indicated that CER, CHOL, and PA mixtures form orthorhombic hydrocarbon chain packing.[14] Thus, the presence of fatty acids appears to be important for the formation of orthorhombic hydrocarbon chain packing. In hairless mouse stratum corneum, the correlation of lamellar structure and hydrocarbon chain packing has been investigated.[6] These correlations of the lipid compositions and microstructure of CER5/CHOL/PA bilayers in each cluster were represented the diversity of the intercellular lipid in stratum corneum. The short lamellar structure of intrinsic intercellular lipids in the stratum corneum, whose repeat distance was about 6 nm, was composed of orthorhombic hydrocarbon chain packing, and the long lamellar structure in native stratum corneum, whose repeat distance was about 13 nm, was composed of hexagonal hydrocarbon chain packing. The present results indicated a similar nature for the hairless mouse stratum corneum, although the repeat distance of the lamellar structure was a little different. It was considered that the intercellular lipid in stratum corneum had two lipid domains, which were hexagonal and orthorhombic hydrocarbon chain packing.

The $R_{\text{Hexa/Ortho}}$ value of human stratum corneum was calculated to be 1.02. The CER5/CHOL/PA bilayers in clusters 1 and 2 were close to the $R_{\text{Hexa/Ortho}}$ value of human stratum corneum. Thus, considering the apparent ratio of the hydrocarbon chain packing, these CER5/CHOL/PA bilayers can be used as appropriate models of the intercellular lipids in the stratum corneum.

In this study, distinguished clusters of CER5/CHOL/PA bilayers were identified for the first time by using RSM-S and SOM. The microstructures of CER5/CHOL/PA bilayers were partially similar to those of intercellular lipids in the stratum corneum, suggesting the usefulness of CER5/CHOL/PA bilayers for understanding the barrier function of the stratum corneum.

Acknowledgments The synchrotron X-ray scattering experiments were performed in a BL15A at the Photon Factory under approval of the Photon Factory Advisory Committee (2008G079) and BL40B2 at the SPring-8 with the approval of the SPring-8 Proposal Review Committee (2009A1876). This work was supported by a grant from the Ministry of Education, Culture, Sports, Science and Technology of Japan. The authors are grateful to the Yamatake Corporation for providing us with dataNESIA® software. We also would like to express our gratitude and deepest appreciation to Assoc. Prof. Hiroshi Takahashi (Gunma University, Department of Biological and Chemical Engineering), Prof. Satoru Kato, and Dr. Masanao Kinoshita (Kwansei Gakuin University, Department of Physics) for their assistance with the SAXS and WAXS measurements and their valuable advice.

References

1) White S. H., Mirejovsky D., King G. I., *Biochemistry*, **27**, 3725—3732 (1988).
2) Bouwstra J. A., Gooris D. S., van der Spek J. A., Lavrijsen S., Bras W., *Biochem. Biophys. Acta*, **1212**, 182—192 (1994).
3) Charalambopoulou G. C., Steriotis T. A., Hauss T., Stubos A. K., Kanelloupoulos N. K., *Physica B*, **350**, e603—e606 (2004).
4) Bouwstra J. A., Gooris G. S., van der Spek J. A., Bras W., *J. Invest. Dermatol.*, **97**, 1005—1012 (1991).
5) Bouwstra J. A., Gooris G. S., Salomons-de Vries M. A., van der Spek J. A., Bras W., *Int. J. Pharm.*, **84**, 205–216 (1992).
6) Hatta I., Ohta N., Inoue K., Yagi N., *Biochem. Biophys. Acta*, **1758**, 1830—1836 (2006).
7) Egawa M., Tagami H., *Br. J. Dermatol.*, **158**, 251—260 (2008).
8) Yagi E., Sakamoto K., Nakagawa K., *J. Invest. Dermatol.*, **127**, 895—899 (2007).
9) Hanson K. M., Behne M. J., Barry N. P., Mauro T. M., Gratton E., Clegg R. M., *Biophys. J.*, **83**, 1682—1690 (2002).
10) Percot A., Lafleur M., *Biophys. J.*, **81**, 2144—2153 (2001).
11) Potts R. O., Golden G. M., Francoeur M. L., Mak V. H. W., Guy R. H., *J. Controlled Release*, **15**, 249—260 (1991).
12) Obata Y., Hatta I., Ohta N., Kunizawa N., Yagi N., Takayama K., *J. Controlled Release*, **115**, 275—279 (2006).
13) Bouwstra J. A., Gooris G. S., Dubbelaar F. E., Weerheim A. M., Ijzerman A. P., Ponec M., *J. Lipid Res.*, **39**, 186—196 (1998).
14) Bouwstra J. A., Gooris G. S., Dubbelaar F. E. R., Ponec M., *J. Invest. Dermatol.*, **118**, 606—617 (2002).
15) Bouwstra J. A., Gooris G. S., Cheng K., Weerheim A., Bras W., Ponec M., *J. Lipid Res.*, **37**, 999—1011 (1996).
16) Watanabe H., Obata Y., Ishida K., Takayama K., *Colloids Surf. B*, **73**,

116—121 (2009).
17) Onuki Y., Takayama K., *J. Colloid Interface Sci.*, (2009), in press.
18) Onuki Y., Ohyama K., Kaseda C., Arai H., Suzuki T., Takayama K., *J. Pharm. Sci.*, **97**, 331—339 (2008).
19) Robson K. J., Stewart M. E., Michelsen S., Lazo N. D., Downing D. T., *J. Lipid Res.*, **35**, 2060—2068 (1994).
20) Weerheim A., Ponec M., *Arch. Dermatol. Res.*, **293**, 191—199 (2001).
21) Wang J., Megha, London E., *Biochemistry*, **43**, 1010—1018 (2004).
22) Golden G. M., McKie J. E., Potts R. O., *J. Pharm. Sci.*, **76**, 25—28 (1987).